

Silicon Germanium Epitaxy: A New Material For MEMS

J.T. Borenstein*, **N.D. Gerrish*†**, **R. White*‡**, **M.T. Currie**** And **E.A. Fitzgerald****

* Charles Stark Draper Laboratory, 555 Technology Square, Cambridge, MA 02139

** Department of Materials Science & Engineering, MIT, 77 Massachusetts Avenue, Cambridge, MA 02139

† Present Address: Amberwave Systems Corporation, Salem, NH

‡ Present Address: Mechanical Engineering Department, University of Michigan, Ann Arbor, MI

ABSTRACT

A wide array of materials have been investigated as candidate fabrication templates for precision microelectromechanical structures, including boron-diffused silicon, boron-doped epitaxial silicon, polysilicon, silicon-on-insulator, and wafer-thick bulk structures. Here we present the latest fabrication results for epitaxial silicon-germanium alloys, a new class of materials which possess excellent crystalline structure, are compatible with non-toxic etchants in bulk micromachining, and are capable of on-chip integration with electronics. For MEMS applications, silicon-germanium alloy layers are grown using a graded buffer approach, resulting in very high quality micromachined structures. Very low defect densities are obtained through the use of these relaxed buffers. Original etch-stop studies determined that Ge doping provided a very weak selectivity in anisotropic etchants such as KOH and EDP. However, by extending the range of Ge concentration to over 20%, we have found extremely high etch selectivities in a variety of etchants. Unlike boron-doped layers, SiGe exhibits etch stop characteristics in the non-toxic, process compatible solution TMAH. The combination of independence from boron doping concentration and etchant compatibility make SiGe a material which is ideal for integration with on-chip electronics.

In this work we present the latest fabrication data on comb-drive resonators built using SiGe epitaxial layers. Process compatibility issues related to wafer curvature, surface finish and reactive-ion-etching chemistries are addressed. An unexpected result of the fabrication process, curvature of released structures, is resolved by annealing wafers after the SiGe deposition. Changes in Young's modulus arising from the high atomic fraction of Ge in the device can be determined by simple beam analysis based on observed resonant frequencies. Overall, build precision for these devices is excellent. We conclude by addressing the remaining challenges for wide-scale implementation of silicon-germanium epitaxial MEMS.

INTRODUCTION

New process technologies for MEMS, including Deep Reactive Ion Etching (DRIE), wafer bonding and Silicon-On-Insulator (SOI) materials, have greatly expanded capabilities for building large, thick and highly precise structures. Over the past few years, we have been developing silicon-germanium epitaxial materials as another technology base for high-precision MEMS structures. Early work by Draper Laboratory demonstrated bulk-micromachined inertial MEMS sensors built from highly-boron-doped crystalline silicon [1]. These devices exhibited excellent performance, but were limited in size and precision by some of the features of the

boron doping process. With this new SiGe technology, it is possible to build thick, large, high-precision structures without boron doping and with low defect densities. Current work is aimed at determining the effects of SiGe process variables on the structural parameters and ultimate performance of MEMS devices. Initial results of a large matrix of SiGe compositions are reported here.

SILICON-GERMANIUM EPITAXY

The use of relaxed buffer layers to produce SiGe films with minimal lattice mismatch and low threading dislocation densities has been described previously [2]. These films are deposited in a UHV-CVD system at temperatures ranging from 550 – 900 °C and pressures of 1 mTorr to 1 Torr. In the present study, a matrix of SiGe epitaxial structures has been produced, with alloy and background doping concentrations and buffer layer parameters as variables. Some compositions do not contain a buffer layer, in order to determine the impact of high lattice strain and residual defect concentrations on specific MEMS structural parameters. Previous studies have determined the impact of SiGe composition on etch selectivity [3]; the focus of the current set of experiments is to study the impact of SiGe composition on structural parameters such as substrate strain, curvature, Young’s modulus, and ultimately on the performance of inertial MEMS sensors.

Full microstructural and compositional characterization of the matrix of SiGe layers has been conducted. Figure 1 shows a TEM image of one of the compositions with the buffer layer shown beneath the device layer. Lattice defect densities in highly-boron-doped layers greatly exceed the concentrations seen in these relaxed buffer layers [4]. Residual defects present in these structures may be responsible for the curvature seen when unannealed films are used to fabricate devices. Spreading Resistance Profiles (SRP) of these films reveals extremely uniform background doping; an SRP profile for the boron doping in the film is shown in Figure 1b. Analysis of the purity and chemical composition of films using SIMS shows that Ge concentrations are also very uniform, that all of the dopants are electrically active, and that the concentrations of other elements are all below detection limits.

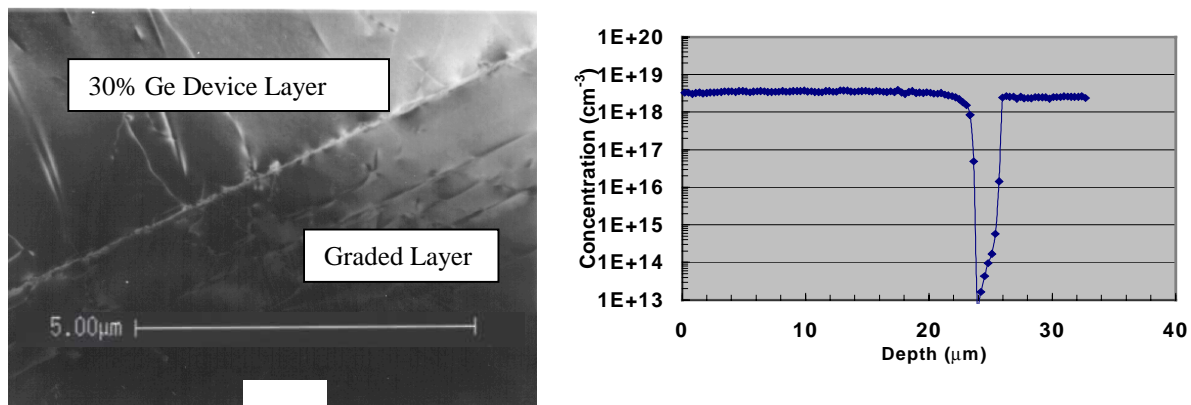


Figure 1. (a) TEM image of $Si_{0.7}Ge_{0.3}$ film with relaxed buffer layer. (b) SRP of boron concentration for the layer, with buffer layer shown as a 2-micron film beneath the device layer.

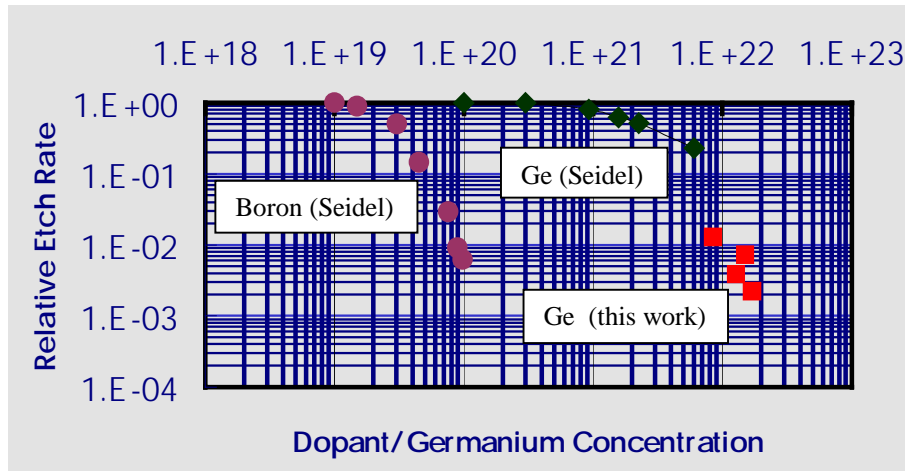


Figure 2. Etch selectivities (squares) of SiGe layers versus Ge concentration, compared with previous studies by Seidel [5] for Ge doping (diamonds) and boron doping (circles.)

Figure 2 illustrates the relationship between etch selectivity and Ge concentration in SiGe alloys with a relaxed buffer layer. As has been previously reported, Ge concentrations in excess of 17% result in very high selectivity in ethylenediamine pyrocatechol (EDP), potassium hydroxide (KOH) and tetramethyl ammonium hydroxide (TMAH) [3]. To our knowledge, SiGe is the only bulk etch stop with a high selectivity in TMAH. Background boron doping has little effect on etch selectivity, and is determined rather by the requirement for conductivity in the MEMS structure. Higher Ge concentrations give rise to higher etch selectivity, and therefore improved build precision, but carry the cost of higher substrate-induced strain and the potential for increased lattice disruption.

MEMS DEVICE RESULTS

A series of comb resonator structures have been built from several of the alloy compositions described above. These include simple comb drive oscillators as well as tuning fork gyroscopes. The fabrication process used to build these devices is virtually identical to the conventional dissolved wafer process described previously [6]. Photolithographic and etching processes are virtually unaffected by the use of SiGe alloys, provided that the surfaces are smooth and the wafers flat. Optically smooth surfaces may be obtained by a light CMP step prior to processing. Wafer flatness, which is essential for processability, may be achieved by careful control of the epitaxial process. Deep Reactive Ion Etching (DRIE) using the Bosch process [7] is not significantly affected by the high germanium concentration. For this set of experiments, the substrates employed were conventional Schott Borofloat wafers. While the anodic bonding process itself was not affected by the SiGe surface, substrate-induced strain increased, as described below. Several options for the wafer dissolution chemistry provide excellent etch-stop characteristics, as was seen in Figure 2. For these experiments we employed EDP and TMAH rather than KOH, a choice driven by compatibility with the metal electrodes. In Figure 3 below we show the high quality surfaces and structures obtained using one of the SiGe epitaxial compositions from the matrix.

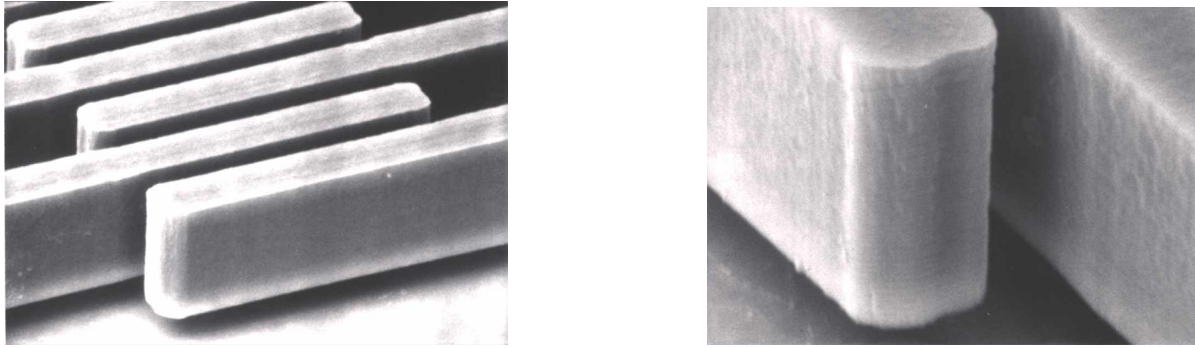


Figure 3. SEM micrograph (left) of section of comb drive showing straight sidewalls and narrow gaps between opposing comb fingers. The tight spacings are indicative of a very high quality etch stop. High magnification image (right) showing the smoothness of sidewalls and lack of defect etching morphology common to highly-boron-doped MEMS structures.

Evaluation of several types of MEMS devices built from SiGe materials involved structural parameters, such as device curvature, substrate strain and etching uniformity, as well as electrical properties including resonant frequencies and quality factors. Here we describe initial results, focusing on three critical parameters, device curvature, device-substrate strain, and the drive resonant frequency of the device. The latter is used to estimate the Young's modulus of silicon-germanium alloys, based on simple beam analysis.

Early efforts to fabricate resonators built from SiGe layers resulted in severely curved suspended structures. This curvature is believed to be due to residual microstructural defects, and it is completely resolved by annealing the layer prior to the fabrication process. An aerial SEM view of the combs is shown in Figure 4, with the anchored comb fingers on the left and the suspended combs on the right. No evidence of disengagement between the pairs of combs is observed. Interferometric measurements [8] of these combs indicates that the maximum disengagement of 10 micron thick structures is $0.08 \mu\text{m}$.

Anodic bonding and wafer bonding processes are typically designed to minimize the residual strain between the structural material and the underlying substrate. In the case of the

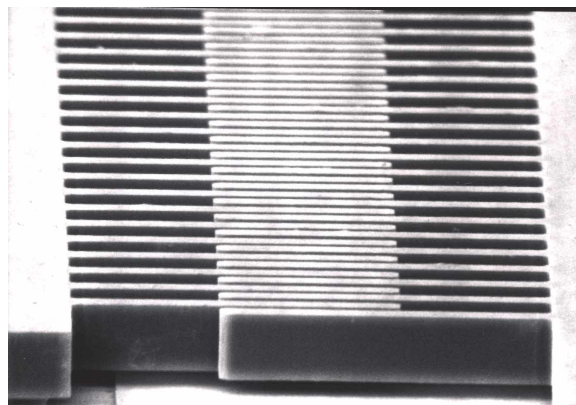


Figure 4. SEM of comb drive showing near-perfect engagement between anchored (left) and suspended comb fingers (right).

dissolved wafer process, glass with a Temperature Coefficient of Expansion (TCE) close to that of silicon is anodically bonded to the device layer. This results in a very low residual strain due to substrate mismatch. Test structures on the tuning fork gyroscope masksets measure substrate-induced strains on the order of 5 – 10 microstrains. The presence of high boron doping appears to have little effect on the strain level. However, SiGe alloys have a significant effect on the strain, since the TCE of alloys with high Ge concentration is greatly increased over the level for silicon. Strain measured by SiGe test structures is more than an order of magnitude greater than that seen in boron-doped silicon counterparts. The effects of this very high substrate-induced strain are presently being assessed.

Tuning fork gyroscopes were fabricated using several of the $\text{Si}_x\text{Ge}_{1-x}$ epitaxial layers described in the present work. Operation of the Draper tuning fork gyroscope has been described separately [9]. One of the primary resonant modes is known as the drive frequency, which is an antisymmetric in-plane motion where the two proof masses move alternately away and towards each other at the same amplitude. The frequency of this mode can be calculated based on knowledge of the Young's modulus, beam width, and material density, along with several smaller effects. Resonant frequency of a beam excited laterally can be written as [10]

$$F_D = C_1 (E w^2 / \rho)^{1/2} \quad (1)$$

where C_1 is a constant depending upon other terms, E is the Young's modulus and ρ the density of the resonator material, and w is the width of the vibrating beam. Other terms affecting resonant frequency, such as drive amplitude, the level of pressure in the evacuated gyro package, and beam thickness, are held constant for all materials studied.

Accurate determination of constitutive values such as the Young's modulus of $\text{Si}_x\text{Ge}_{1-x}$ layers will require a large number of measurements in a carefully controlled experiment [11]. Such analysis is now underway, pending completion of the large process matrix now in progress. Preliminary data emerging from this analysis suggests that the Young's modulus of the $\text{Si}_x\text{Ge}_{1-x}$ layers closely matches a linear extrapolation between values for pure Si and Ge. Resonator beam width, as measured by scanning electron microscopy, varies significantly between materials. Superior etch stop properties cause the SiGe beams to be roughly one micron wider than Si:B doped counterparts. However, the geometric stiffening effect of wider $\text{Si}_x\text{Ge}_{1-x}$ beams is offset by the higher density of silicon-germanium alloys, and by a lower Young's modulus. This offset results in relatively small net shifts in modal frequency. Density is estimated by invoking Vegard's Law [12], which assumes that the lattice constant varies linearly with composition. Values for Young's modulus for Si and Ge are taken from the 1965 paper of Wortman and Evans [13]. This analysis predicts a motor frequency ratio of the $\text{Si}_{0.7}\text{Ge}_{0.3}$ / Si compositions of 0.88, which compares favorably with an observed ratio of 0.90 based on a sample of six gyro devices.

CONCLUSIONS

Preliminary fabrication and device results using several of the SiGe materials investigated in this study are very encouraging. When compared with alternative materials, such as boron-diffused silicon, epitaxial boron-doped silicon, and SOI layers, silicon-germanium alloys exhibit many advantages. Four basic figures of merit useful for evaluating single-crystal

MEMS materials are: 1) Etch-stop properties, 2) Processing issues, 3) Safety and environmental considerations, and 4) Compatibility with on-chip integration of electronics. It has already been shown [14] that SiGe alloys have superior etch-stop properties to boron-doped etch stops, as does the etch stop on oxide in SOI processing. Based on environmental/safety considerations, SiGe (and SOI) are preferred, since they do not require the use of hazardous EDP. Both SiGe and SOI are compatible with on-chip electronics, while boron-doped layers are not. Finally, processing issues such as defects, curvature and thickness limits do not hinder SiGe and SOI materials as they do highly-boron-doped layers. For SiGe alloys, the primary remaining process issue is the strain between the structural layer and the underlying substrate. Current efforts are focused on completing the process matrix to determine the influence of critical SiGe device and buffer layer parameters on residual strain, etch stop properties and resonator performance.

REFERENCES

1. A. Kourepenis, J. Borenstein, J. Connelly, R. Elliott, P. Ward and M. Weinberg in *IEEE Position, Location and Navigation Symposium*, (IEEE, Palm Springs CA, 1998), pp. 1-8.
2. E. A. Fitzgerald, K. C. Wu, M. Currie, N. Gerrish, D. Bruce, and J. T. Borenstein in *Microelectromechanical Structures for Materials Research*, edited by S. Brown, J. Gilbert, H. Gückel, R. Howe, G. Johnston, P. Krulevitch and C. Muhlstein, (Mater. Res. Soc. Proc. **518**, Pittsburgh, PA, 1998) pp. 233-238.
3. J. T. Borenstein, N. D. Gerrish, M. T. Currie and E. A. Fitzgerald, in *Materials Science of Microelectromechanical Systems (MEMS) Devices*, edited by A.H. Heuer and S.J. Jacobs, (Mater. Res. Soc. Proc. **546**, Pittsburgh, PA, 1999) pp. 69-74.
4. K.C. Wu, P.A. Shay, J.T. Borenstein and E.A. Fitzgerald in *Materials for Mechanical and Optical Microsystems*, edited by M.L. Reed, M. Elwenspoek, S. Johansson, E. Obermeier, H. Fujita and Y. Uenishi, (Mater. Res. Soc. Proc. **444**, Pittsburgh, PA, 1997) pp. 197-202 .
5. H. Seidel, L. Csepregi, A. Heuberger and H. Baumgärtel, *J. Electrochem. Soc.*, **137** 3626 (1990.)
6. S.T. Cho, in *Micromachining and Microfabrication Process Technology*, edited by K.W. Markus, (SPIE Press, Vol. **2639**, Bellingham, WA, 1995) pp. 10-17.
7. A.A. Ayon, K.-S. Chen, K.A. Lohner, S.M. Spearing, H.H. Sawin and M.A. Schmidt in *Materials Science of Microelectromechanical Systems (MEMS) Devices*, edited by A.H. Heuer and S.J. Jacobs, (Mater. Res. Soc. Proc. **546**, Pittsburgh, PA, 1999) pp. 51-62.
8. J. T. Borenstein, P. Greiff, J.B. Sohn and M.S. Weinberg in *Micromachining and Microfabrication Process Technology II*, edited by S.W. Pang and S.-C. Chang, (SPIE Press, Vol. **2879**, Bellingham, WA, 1996) pp. 116-125.
9. J. Bernstein, S. Cho, A.T. King, A. Kourepenis, P. Maciel and M. Weinberg in *Proc. of the IEEE MEMS Workshop*, edited by A. Pisano and J. Lang, (IEEE, 1993) pp. 143-148.
10. W.C.C. Young and R.J. Roark, *Roark's Formulas for Stress and Strain*, 6th ed., (McGraw-Hill, New York, 1990.)
11. S.D. Senturia, this proceedings.
12. L. Vegard, *Z. Phys.*, **5** 17 (1921.)
13. J.J. Wortman and R.A. Evans, *J. Appl. Phys.* **36** 153 (1965.)
14. J. T. Borenstein, N. D. Gerrish, M. T. Currie and Fitzgerald in *Proc. of 12th Intl. Workshop on MEMS*, edited by K. Gabriel and K. Najafi, (IEEE, Orlando, FL, 1999), pp. 205-210.